Molecular Biology of the Cell
Vol. 18, 3607–3619, September 2007

LEKTI Fragments Specifically Inhibit KLK5, KLK7, and KLK14 and Control Desquamation through a pH-dependent Interaction[D]

Celine Deraison,*†‡§ Chrystelle Bonnart,*†§ Frederic Lopez,‖ Celine Besson,*† Ross Robinson,¶ Arumugam Jayakumar,# Fredrik Wagberg,@ Maria Brattsand, Jean Pierre Hachem,†† Goran Leonardsson,@ and Alain Hovnanian*†‡**

*Institut National de la Santé et de la Recherche Médicale, U563, Toulouse, F-31300 France; †Université Toulouse III Paul-Sabatier, Unité Mixte de Recherche-S563, Toulouse, F-31400 France; ‡Centre Hospitalier Universitaire de Toulouse, Hopital Purpan, Departement de Génétique Médicale, Toulouse, F-31000 France; ‖Université Toulouse III Paul-Sabatier, Faculté de Médecine Toulouse-Rangueil, Institut Louis Bugnard (IFR31), Toulouse, F-31400 France; ¶Wellcome Trust Centre for Human Genetics, Oxford OX3 7BN, United Kingdom; #Department of Head and Neck Surgery, M. D. Anderson Cancer Center, Houston, TX 77030; @Arexis AB/Biovitrum, 413 46 Gothenburg, Sweden; **Department of Public Health and Clinical Medicine, Section for Dermatology and Venereology, Umeå University, SE-901 87 Umeå, Sweden; and ††Department of Dermatology, Vrije Universiteit Brussels, 1090 Brussels, Belgium

Submitted February 14, 2007; Revised June 11, 2007; Accepted June 18, 2007
Monitoring Editor: M. Bishr Omary

LEKTI is a 15-domain serine proteinase inhibitor whose defective expression underlies the severe autosomal recessive ichthyosiform skin disease, Netherton syndrome. Here, we show that LEKTI is produced as a precursor rapidly cleaved by furin, generating a variety of single or multidomain LEKTI fragments secreted in cultured keratinocytes and in the epidermis. The identity of these biological fragments (D1, D5, D6, D8–D11, and D9–D15) was inferred from biochemical analysis, using a panel of LEKTI antibodies. The functional inhibitory capacity of each fragment was tested on a panel of serine proteases. All LEKTI fragments, except D1, showed specific and differential inhibition of human kallikreins 5, 7, and 14. The strongest inhibition was observed with D8–D11, toward KLK5. Kinetics analysis revealed that this interaction is rapid and irreversible, reflecting an extremely tight binding complex. We demonstrated that pH variations govern this interaction, leading to the release of active KLK5 from the complex at acidic pH. These results identify KLK5, a key actor of the desquamation process, as the major target of LEKTI. They disclose a new mechanism of skin homeostasis by which the epidermal pH gradient allows precisely regulated KLK5 activity and corneodesmosomal cleavage in the most superficial layers of the stratum corneum.

INTRODUCTION

Lympho-epithelial Kazal type inhibitor (LEKTI), is encoded by *SPINK5* (Serine Proteinase Inhibitor Kazal type 5) (Magert *et al.,* 1999). LEKTI, belongs to the Kazal serine proteinase inhibitor family whose numerous members generally bear 3–7 tandem kazal domains. Interestingly, LEKTI contains a signal peptide and exhibits as many as 15 potential serine proteinase inhibitory domains (D1–D15) separated by 14 spacing segments. These linker regions are characterized by the presence of several dibasic residues, potentially sensitive to the cleavage by the subtilisin-like proprotein convertases. Two of these domains (D2 and D15) resemble typical Kazal-type serine proteinase inhibitors, as deduced from their primary structure and characteristic pattern of six cysteine residues. The other 13 domains share high homology with this class of inhibitors but lack one of the three conserved typical disulfide bridges. Despite this difference, these sequences adopt a hairpin structure, creating an inhibitory binding loop (Lauber *et al.,* 2003). Several authors have studied the inhibitory capacity of different forms of LEKTI. The full-length LEKTI recombinant protein has been shown to inhibit trypsin, subtilisin A, plasmin, cathepsin G, and neutrophil elastase, but not chymotrypsin (Mitsudo *et al.,* 2003). A partial recombinant form of LEKTI containing domains 6–9 (rLEKTI6–9) has been shown to inhibit trypsin, subtilisin A, chymotrypsin, kallikrein 5 (KLK5, stratum corneum tryptic enzyme [SCTE]), and kallikrein 7 (KLK7, stratum corneum chymotryptic enzyme [SCCE]) but not plasmin, cathepsin G, or elastase (Jayakumar *et al.,* 2004; Schechter *et al.,* 2005). In addition, the single domain D6 was shown to be a potent inhibitor of trypsin, KLK5, and KLK7, whereas D15 was not effective against these two kallikreins

This article was published online ahead of print in *MBC in Press* (http://www.molbiolcell.org/cgi/doi/10.1091/mbc.E07–02–0124) on June 27, 2007.

[D] The online version of this article contains supplemental material at *MBC Online* (http://www.molbiolcell.org).

§ These authors contributed equally to this work.

Address correspondence to: Alain Hovnanian (alain.hovnanian@toulouse.inserm.fr).

Abbreviations used: BIA, biomolecular interaction analysis; CHO, Chinese hamster ovary; GR, granular layer; HBS, HEPES-buffered saline; KLK, kallikrein; LEKTI, Lympho-epithelial Kazal type inhibitor; $LEKTI_{f\text{-}l}$, full-length LEKTI; $LEKTI_{sh}$, short-length LEKTI; NHK, normal human keratinocytes; NS, Netherton syndrome; SC, stratum corneum; SPINK5, serine proteinase inhibitor Kazal type 5.

(Egelrud *et al.*, 2005). Altogether, these results highlight the fact that each form of LEKTI exhibits its own inhibitory specificity.

LEKTI is expressed specifically in the most differentiated viable layers of stratified epithelial tissues and in the Hassal corpuscules of the thymus (Bitoun *et al.*, 2003). In the epidermis, it is mainly restricted to the granular layer (GR), where critical biochemical and morphological changes that occur during terminal differentiation lead to cornification (stratum corneum [SC] formation). LEKTI is transported by specific intracellular lamellar granule cargoes until its secretion in the extracellular space, between granular cells and cornified cells (Ishida-Yamamoto *et al.*, 2005).

In normal human keratinocytes (NHK), LEKTI is expressed as three precursors derived from alternative pre-mRNA processing (Tartaglia-Polcini *et al.*, 2006). In addition to the previously described, full-length isoform of 15 domains (145 kDa), *SPINK5* encodes a shorter LEKTI isoform (125 kDa) composed of the first 13 domains generated from the use of an alternative polyadenylation signal, as well as a longer isoform (148 kDa) carrying a 30-amino acid residue insertion between the 13th and the 14th inhibitory domains, generated from the activation of cryptic splice junction sequences. RNase protection assay experiments have identified the full-length transcript as the most abundant isoform in NHK (Tartaglia-Polcini *et al.*, 2006). LEKTI precursors are rapidly processed into proteolytic fragments in a postendoplasmic reticulum compartment (Bitoun *et al.*, 2003; Jayakumar *et al.*, 2005). C-terminal LEKTI fragments have been detected in the conditioned medium of NHK (Tartaglia-Polcini *et al.*, 2006). In addition, a 30-kDa polypeptide with an N-terminal extremity, corresponding to D8, has also been purified from NHK-conditioned medium (Ahmed *et al.*, 2001).

SPINK5 mutations lead to Netherton syndrome (NS; Chavanas *et al.*, 2000), a severe autosomal recessive skin disorder characterized by congenital ichthyosiform erythroderma, a specific hair shaft defect (trichorrhexis invaginata) and atopic manifestations (Traupe, 1989). To decipher the biological functions of LEKTI, we have genetically engineered mice with a targeted disruption of *Spink5*. *Spink5*-null mice faithfully replicate key features of Netherton syndrome, including abnormal desquamation, impaired keratinization, hair malformation, and a severe skin barrier defect. LEKTI deficiency causes abnormal desmosome cleavage in the upper GL through desmoglein 1 degradation due to the hyperactivity of KLK5 and KLK7. This leads to accelerated SC shedding and consequent loss of skin barrier function (Yang *et al.*, 2004; Descargues *et al.*, 2005; Hewett *et al.*, 2005). This work identified LEKTI as a key regulator of epidermal protease activity. In addition, the presence of LEKTI domains (D1, D5, and D6) in the blood circulation (Magert *et al.*, 1999, 2002) suggests that LEKTI could also have biological effects at a distance from the skin. The extent of atopic manifestations in NS predicts a role for LEKTI as an inhibitor of proteases involved in the inflammation process.

To gain further insight into LEKTI functions, we studied the inhibitory properties of physiological LEKTI fragments. The different LEKTI forms present in the epidermis, in NHK, as well as in a mammalian heterologous expression system were detected using three antibodies directed against the N-terminal, the internal and the C-terminal part of full-length LEKTI. We produced several of these physiological LEKTI proteolytic fragments and characterized their inhibitory properties against a large panel of serine proteinases involved in skin homeostasis and inflammation. Kinetic parameters of the interaction between LEKTI fragments and their proteinase targets were studied by surface plasmon resonance (SPR). Using the same technology, we showed that the pH gradient occurring through the SC controls the interaction strength between LEKTI and KLK5, thus allowing the controlled release of active proteinase in the most superficial layers of SC.

MATERIALS AND METHODS

Antibodies, Proteinases, and Substrates

Anti-LEKTI antibodies used in this study were as follows: a rabbit polyclonal antibody raised against D1–D6 LEKTI domains (Bitoun *et al.*, 2003), a rabbit polyclonal antibody raised against D8–D11 LEKTI domains (Ishida-Yamamoto *et al.*, 2005) and a rabbit polyclonal antibody raised against D13–D15 LEKTI domains (Bitoun *et al.*, 2003). Trypsin, tryptase, chymotrypsin, plasmin, thrombin, neutrophile elastase, cathepsin G, and kallikreins 1 and 3 were purchased from Sigma-Aldrich (St. Louis, MO). KLK8 was purchased from R&D Systems (Minneapolis, MN). Recombinant kallikreins KLK5, KLK7, and KLK14 were obtained as previously described (Brattsand *et al.*, 2005). All chromogenic substrates were commercially obtained (Sigma-Aldrich).

Human Epidermis and Cell Culture

Normal and NS human primary keratinocytes were isolated from skin biopsies and cultured in Green medium containing 1.2 mM calcium as previously described (Bitoun *et al.*, 2003). Chinese hamster ovary (CHO) and furin-deficient CHO cells were a generous gift of Dr. Leppla (Laboratory of Microbial Ecology, National Institute of Dental Research, NIH, Bethesda, MD 20892) (Gordon *et al.*, 1995). Cells were grown in F12 medium (Invitrogen, Carlsbad, CA) supplemented with 10% fetal calf serum and 100 U/ml penicillin/streptomycin. Human foreskin was obtained after medical surgery at Purpan Hospital (Toulouse, France). The epidermis was mechanically separated from the dermis after heating at 55°C for 15 min. The medical ethical committee CCPPRB (Comité consultatif de personnes se prêtant à des recherches biomédicales) of Toulouse hospitals approved all described studies (research project no. 0102908). The study was conducted according to the Declaration of Helsinki principles.

Cloning, Expression, and Purification of LEKTI Domains

Partial LEKTI cDNA fragments encoding the following human LEKTI fragments: D1 (residues 23-77), D5 (residues 292-353), D6 (residues 356-423), and D8–D11 (residues 490-759) were amplified by PCR from a vector containing the full-length cDNA as a template; amino acid numbering is according to Magert *et al.* (1999). PCR products of D5 and D6 were cloned into pGEX in order to use glutathione *S*-transferase (GST) as a C-terminal tag. D1 and D8–D11 PCR products were cloned into pET22b, to introduce an in-frame N-terminal His_6 tag. All the constructs were transformed into the Origami bacterial strain (Novagen, Madison, WI) in order to produce recombinant LEKTI fragments. Previous studies have demonstrated that similar prokaryotic expression systems are suitable to obtain functional LEKTI fragments (Kreutzmann *et al.*, 2004; Egelrud *et al.*, 2005).

Production of recombinant LEKTI fragments was induced by adding 1 mM isopropyl-1-thio-β-D-galactopyranoside (IPTG) to Origami cultures (Novagen). After 3 h at 30°C, cells were harvested, lysed in PBS containing 0.1 mM EGTA, 0.25% Tween 20, 100 μg/ml lysosyme, and subjected to sonication for optimal solubilization. For GST fusion proteins, the soluble fraction was loaded onto a glutathione Sepharose 4B column according to the recommendations of the MicroSpin GST purification module (GE Healthcare, Waukesha, WI). For His-fusion proteins, the soluble fraction was subjected to nickel affinity (Chelating Sepharose Fast Flow, GE Healthcare, Waukesha, WI). Elution was performed using a gradient of imidazole (0–500 mM in PBS) on fast protein liquid chromatography (FPLC). Nickel-eluted fractions were subsequently loaded onto a cation exchange column (SP Sepharose High performance, GE Healthcare), for which a gradient of NaCl (0–2 M) was carried out to elute proteins. Finally, size exclusion chromatography (HiLoad 16/60 Superdex 75 pq, GE Healthcare) was used to obtain pure protein fractions, which were pooled for further experiments. Purified proteins were analyzed by SDS-PAGE after Coomassie Blue staining. HisD9–D15 was purified following the experimental procedures as previously described (Jayakumar *et al.*, 2004). Proteins were dialyzed against a solution of HEPES 10 mM, pH 7.4, for inhibitory activity assay and Biacore analysis.

Cloning of LEKTI cDNAs into pEF-DEST51 Expression Vector

LEKTI full-length cDNA (GenBank NM_006846) or LEKTI short-length (GenBank DQ149929) were amplified by long-range PCR (PfU Turbo, Stratagene, La Jolla, CA) from a vector containing the full-length cDNA as a template. The PCR products were subcloned into pDEST8 vector by homologous recombination and transferred into the mammalian expression vector pEF-DEST51 using the Gateway technology, according to the manufacturer's instructions (Invitrogen). pEF-DEST51-$SPINK5_{f\text{-}l}$ and pEF-DEST51-$SPINK5_{sh}$ constructs were fully sequenced using the Big Dye Terminator Sequencing Kit and an ABI 3100 automated sequencer (Applied Biosystems, Foster City, CA).

CHO Cell Transfections

One day before transfection, CHO cells were plated at 5×10^4 cells per well of a six-well plate. The day of the transfection, cells at 70% confluence were transiently transfected with 1 μg of pEF-DEST51, pEF-DEST51-SPINK5$_{f\text{-}l}$, or pEF-DEST51-SPINK5$_{sh}$ plasmid DNAs, using the FuGENE 6 Transfection Reagent, according to the manufacturer's recommendations (Roche Applied Science, Indianapolis, IN). Twenty-four hours after transfection, the medium was replaced with serum-free medium, and cells were maintained in culture for an additional 24 h. Both intracellular and extracellular protein extracts were prepared for Western blot analysis.

Western Blotting

Epidermis was crushed in a protein extraction buffer (PEB) containing Tris-Cl 50 mM, pH 8, NaCl 150 mM, EDTA 5 mM, pH 8, 1% NP40, 1 mM PMSF, 10 μg/ml leupeptin, 10 mg/ml pepstatin A, and 1 mg/ml antipain with an Ultra-Turrax. Cultured cells were lysed in PEB. Lysates were clarified from insoluble material by centrifugation at 13000 *g*, 4°C for 5 min. The conditioned medium was concentrated by overnight acetone precipitation. Proteins were recovered by centrifugation at 13000 *g*, 4°C for 30 min, and resuspended in lysis buffer. Proteins were quantified by Bradford protein assay kit (Bio-Rad Laboratories, Hercules, CA). Protein fractions were mixed with Laemmli buffer (Bio-Rad Laboratories), incubated for 5 min at 65°C, and then separated by SDS-PAGE. After migration, proteins were transferred to Hybond-C extra membranes (GE Healthcare). After incubation with primary and secondary antibodies, enhanced chemiluminescence detection was performed as recommended by the manufacturer. PNGase F (New England Biolabs, Beverly, MA), *O*-glycosidase, and α-(2→3,6,8,9)-neuraminidase (Sigma-Aldrich) treatments were performed at 37°C, according to the manufacturer's instructions.

Proteinase Activity Assay

Varying concentrations of substrates (Table 1) were incubated with a fixed amount of proteinase in a suitable buffer activity, and initial velocities were measured by monitoring the absorbance at 405 nm. Double reciprocal Lineweaver-Burke plots of 1/[V] versus 1/[S] were used to determine the K_m of each substrate for its partner enzyme. Affinity constant (K_m) between an enzyme and a substrate is defined as the substrate concentrate at 1/2 maximum velocity. Six separate mixtures of enzymes and inhibitors in various ratios were incubated for 5 min. The proteinase activity was initiated by adding the appropriate synthetic substrate (Table 1), and the activity of free enzyme was determined spectrophotometrically at 405 nm by monitoring the release of *p*-nitrophenyl acetate (pNA). All time courses were performed at 25°C, during 15 min, in duplicate. Reaction velocities were linear over the course of the reaction. Initial velocities were measured by monitoring absorbance at 405 nm, and IC_{50} was calculated by plotting $[V_0/V_i]$-1 versus [I]. To account for the effect of substrate K_m on the inhibition constant, IC_{50} were converted to K_i using the formula (Morris *et al.*, 2002):

$$K_i = \frac{IC_{50}}{1 + \frac{[S]}{K_m}}$$

For KLK8, the proenzyme was activated following the manufacturer's instructions and the initial velocity was measured by monitoring fluorescence emission using the Val-Pro-Arg-AMC (Amino 4 Methyl Coumarine) substrate (Ex, 355 nm; Em, 460 nm).

Surface Plasmon Resonance Analysis

Principle. Binding events between two molecules are monitored in real time, without the use of any label, using an optical phenomenon called SPR. Biomolecular binding events cause changes in the refractive index close to the surface layer of a chip, which are detected as changes in the SPR signal. During a binding analysis SPR changes occur as a solution is passed over the surface of a sensorchip. To perform an analysis, one interactant (ligand) is immobilized over a carboxymethylated dextran matrix of a sensorchip. The sensor surface forms one wall of a flow cell. Sample containing the other interactant (analyte) is injected over this surface in a precisely controlled flow. The progress of an interaction is monitored as a sensorgram that expresses resonance units (RU) as a function of time. Analyte binds to the surface-attached ligand during sample injection, resulting in an increase in signal. At the end of the injection, the sample is replaced by a continuous flow of buffer, and the decrease in signal reflects dissociation of interactant from the surface-bound complex.

Materials. All binding studies based on SPR phenomenon were performed on a four-channel BIACORE 3000 optical biosensor instrument (BIAcore AB, Uppsala, Sweden). All experiments were performed on sensorchips CM5 obtained from Biacore AB.

Immobilization of Recombinant LEKTI Domains. Both flow cells of a CM5 sensor chip were coated with recombinant proteins by amine coupling, allowing immobilization of the proteins in the same orientation, independent of the tag fused to the protein. Various levels of RU were immobilized to take into account the differences in molecular weights: His-D1 (500 RU), GST-D5 (2100 RU), GST-D6 (2100 RU), His-D8–D11 (2000 RU), and His-D9-D15 (3800 RU).

BIA Analysis. Binding analyses were performed with multiple injections of different protein concentrations over the immobilized surfaces at 15°C. All samples were diluted in HBS-EP buffer (HEPES 10 mM, NaCl 150 mM, EDTA 3 mM, and polysorbate 0.005%) and were injected over the sensor surface for 3 min at a flow rate of 30 μl/min. All diluted samples were injected at the same time over the four channels (flow cells). A gradient of 0.05% to 0.5% SDS in HBS-EP buffer was used to regenerate the chip. D1 was considered as a negative control according to its inability to affect proteinase activity. D1 sensorgrams were subtracted from sensorgrams obtained with immobilized fusion proteins to yield true binding responses. Kinetics constants (k_a, k_d, $K_D = k_d/k_a$) were calculated using BIAevaluation 4.0.1 software and the 1/1 Langmuir binding model was chosen. This model determines the association constant (k_a) and takes into account the dissociation occurring during the association phase. Therefore, the calculated values do not necessary correlate with apparent slope of the sensorgram.

Casein Gel Zymography

Epidermis from wild-type (WT) and knockout (KO) animals was crushed in 1 M acetic acid solution with an Ultra-Turrax. After overnight extraction at 4°C, soluble proteins were lyophilized and resuspended in PBS. After acetone precipitation, proteins were assayed (Bradford, Bio-Rad), and 5 μg of soluble fractions were mixed in a nondenaturing loading buffer (50 mM Tris-HCl, pH

Table 1. Enzymes, substrates, buffers, and K_m

Proteinase	Substrate	Buffer	K_m
hKLK (75 nM)	Ile-Pro-Arg-pNA (1 mM)	0.1 M Tris, 0.5 M NaCl, pH 8	0.6 mM
hKLK7 (180 nM)	Arg-Pro-Tyr-pNa (1 mM)	137 mM NaCl, 27 mM KCl, 10 nM NaP, pH 7.4	1 mM
hKLK14 (9.4 nM)	Pro-Phe-Arg-pNA (1 mM)	0.1 M Tris, 0.5 M NaCl, pH 8	0.75 mM
hKLK8 (3.2 nM)	Val-Pro-Arg-AMC (0.1 mM)	0.1 M Tris, pH 9	1 mM
hCatG (60 nM)	$(Ala)_2$-Pro-Phe-pNa (0.06 mM)	137 mM NaCl, 27 mM KCl, 10 mM NaP, pH 7.4	1.3 mM
Bovine Trypsin (42 nM)	Nα-Benzoyl-Arg-pNA (2.5 mM)	50 mM Tris, pH 8, 20 mM $CaCl_2$	0.7 mM
Bovine Chymotrypsin (2 nM)	Suc-$(Ala)_2$-Pro-Arg-pNA (0.2 mM)	50 mM Tris, pH 8, 20 mM $CaCl_2$	0.01 mM
hTryptase (8 nM)	Z-Gly-Pro-Arg-pNA (0.2 mM)	50 mM HEPES, 120 mM NaCl	0.05 mM
hElastase (15 nM)	Suc-(Ala)3-pNA (1 mM)	50 mM Tris, pH 8	2 mM
hPlasmin (22.5 pM)	Tosyl-Gly-Pro-Lys-pNA (1 mM)	100 mM Tris, pH 7.6, 120 mM NaCl	3.8 mM
Porcine KLK1 (20 nM)	Val-Leu-Arg-pNA (0.375 mM)	50 mM Tris, pH 7.8, 200 mM NaCl	0.08 mM
hKLK3 (20 nM)	Tosyl-Gly-Pro-Lys-pNa (0.375 mM)	50 mM Tris, pH 9, 200 mM NaCl	0.1 mM
hThrombin (410 nM)	Phe-Val-Arg-pNA (1.5 mM)	100 mM Tris, pH 8, 100 mM NaCl	0.15 mM

For protease activity assay, concentrations of enzymes and their appropriate substrates are indicated, as well as buffer concentration. Affinity constants (K_m) of the enzyme for its substrate have been calculated.

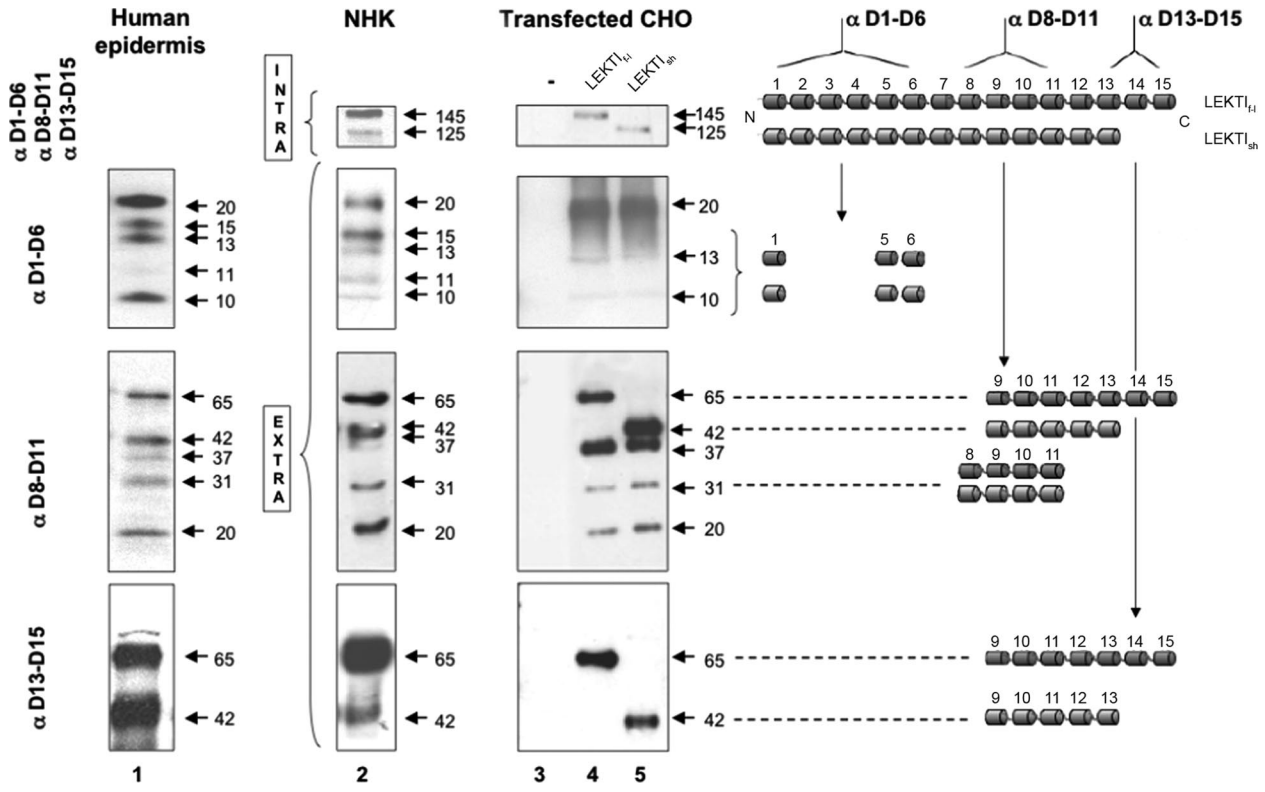

Figure 1. LEKTI proteolytic fragments in the epidermis, normal human keratinocytes, and transfected CHO - Model of LEKTI proteolysis. Protein extracts from human foreskin epidermis (lane 1), cultured normal human keratinocytes (lane 2), or transfected CHO cells (lanes 3–5) were analyzed by Western-blot using three anti-LEKTI antibodies indicated on the left. CHO cells were transiently transfected with the empty pEF-DEST51 vector (−, lane 3); pEF-DEST51-SPINK5$_{f-l}$ (LEKTI$_{f-l}$, lane 4); or pEF-DEST51-SPINK5$_{sh}$ (LEKTI$_{sh}$, lane 5). Intracellular and extracellular fractions of cultured cells were analyzed. The molecular weights of the different bands obtained are indicated in kDa. In intracellular fractions of NHK and transfected CHO, precursors of 145 and 125 kDa are observed with each antibody. Conversely, in the epidermis and in extracellular fractions of NHK and CHO, only proteolytic fragments of LEKTI are visualized. For each antibody used, the molecular weight of these proteolytic LEKTI fragments is indicated. Note the absence of LEKTI precursors detected in human epidermis. Right, schematic representation of LEKTI processing in human epidermis and NHK. A schematic representation of LEKTI processing in human epidermis and NHK is proposed according to the results obtained with the different antibodies used. The two LEKTI precursors (145 and 125 kDa) are processed into several physiological LEKTI fragments. The identity of some LEKTI fragments was proposed according to several parameters, including the antibody used, the molecular weight of the unglycosylated forms (see Figure 3), and the existence of LEKTI fragments already published.

6.8, 2% SDS, 10% glycerol, and 0.1% bromophenol blue) were loaded onto casein copolymerized with acrylamide gels (15% acrylamide, 0.05% α-casein, Sigma-Aldrich) for electrophoresis. Gels were washed with 2.5% Triton X-100 for 1 h to remove SDS and incubated 24 h at 37°C in a reaction buffer containing 50 mM Tris, pH 8. Gels were stained with 1% Coomassie Brilliant blue for 30 min. Areas of caseinolytic activity appeared as clear zones against a dark blue background. To assess inhibitory capacity of D8–D11 LEKTI domain, a solution of D8–D11 fragment (5 μM) was added to the sample before electrophoresis (15 min on ice), as well as in the reaction buffer.

In Situ Zymography

Frozen sections of WT or *Spink5*$^{-/-}$ mouse skin (5-mm thickness) were rinsed with a washing solution (2% Tween 20 in deionized water) and incubated at 37°C overnight with 100 μl of BODIPY FL casein using the EnzChek Ultra Protease Assay kit (Invitrogen) in 50 mM Tris-Cl, pH 8, in order to visualize global protease activity. Cryostat sections were incubated in the same conditions with 100 μl of Boc-Val-ProArg-AMC or Suc-Leu-Leu-Val-Tyr-AMC (Sigma-Aldrich) at 100 mM in Tris 50 mM, $CaCl_2$ 10 mM for the detection of trypsin- and chymotrypsin-like activity, respectively. For some sections, LEKTI D8–D11 fragment (5 μM) was added to the substrate in order to assess its inhibitory capacity. All sections were rinsed with PBS solution and visualized with the inverted high-end microscope Axiovert 200 (Zeiss, Thornwood, NY) at an excitation wavelength of 485 and 400 nm and an emission wavelength of 530 and 460 nm for BODIPY FL and AMC fluorescent dyes, respectively. Frozen sections from WT and KO skin were photographed at equal time points and exposure time. Images were captured and analyzed with Metamorph Imaging system software, version 3.6 (Universal Imaging, West Chester, PA). The intensity of the fluorescence signals was coded as color gradient, ranging from 0 (dark) to 255 (white).

RESULTS

Human Epidermis and Cultured Keratinocytes Secrete LEKTI Proteolytic Fragments after Intracellular Processing of LEKTI Precursors

To detect the presence of LEKTI precursors and proteolytic fragments in human epidermis, foreskin protein extracts were analyzed by Western blotting using three LEKTI antibodies (αD1–D6, αD8–D11, and αD13–D15; Figure 1, lane 1). The same analysis was carried out using intracellular and extracellular fractions of differentiated normal human keratinocytes in culture (NHK; Figure 1, lane 2). Signal specificity was confirmed using extracts of NS keratinocytes, which do not express LEKTI (Bitoun *et al.*, 2003; data not shown).

Bands of 145 and 125 kDa were detected in the intracellular fraction of NHK, with each of the three antibodies (Figure 1, lane 2). These proteins correspond to the full-length (LEKTI$_{f-l}$) and short-length (LEKTI$_{sh}$) LEKTI precursors (Tartaglia-Polcini *et al.*, 2006), respectively, and were not detected in human epidermal extracts.

LEKTI fragments of 10, 11, 13, 15, and 20 kDa were detected in human epidermis with αD1–D6 antibodies (Figure 1, lane 1). The same bands were detected only in the extracellular fraction of NHK, which indicated that these LEKTI N-terminal fragments are secreted (Figure 1, lane 2). Using αD8–D11 antibodies, 20-, 31-, 37-, 42-, and 65-kDa proteolytic fragments were detected in human epidermis and in the conditioned medium of NHK (Figure 1, lanes 1 and 2).

In the epidermis and in the extracellular fraction of NHK, αD13–D15 antibodies detected two C-terminal fragments at ~65 and 42 kDa (Figure 1, lanes 1 and 2). Altogether, these results highlight a similar proteolytic processing of LEKTI in human epidermis in vivo and in NHK in vitro. They also demonstrate the heterogeneity in molecular weights of LEKTI proteolytic fragments. In the C-terminal part of LEKTI, high-molecular-weight proteolytic fragments were produced (65 or 42 kDa) and were not cleaved in a larger extent, in contrast to N-terminal extremity, the proteolytic processing of which produced several small LEKTI fragments.

No LEKTI precursor could be detected in the epidermis with any of the LEKTI antibodies used, suggesting that they are rapidly processed into proteolytic fragments. The fact that LEKTI precursors were detected only in the intracellular fraction of NHK and that LEKTI proteolytic fragments were observed exclusively in the extracellular fraction confirms that LEKTI processing takes place intracellularly (Bitoun *et al.*, 2003) and suggests a rapid secretion of fragments upon cleavage of the precursors. These observations support the notion that secreted LEKTI fragments are the relevant LEKTI biologically active forms.

Heterologous Expression of LEKTI in CHO Cells Reproduces Physiological LEKTI Processing

To discriminate LEKTI fragments deriving from the full-length LEKTI precursor from those deriving from the shorter LEKTI precursor, we developed an heterologous system for LEKTI expression. Transient transfection of CHO cells was performed with mammalian expression vectors carrying the full-length (pEF-DEST51-LEKTI$_{f\text{-}l}$) or short-length (pEF-DEST51-LEKTI$_{sh}$) LEKTI cDNAs under the control of the Elongation Factor 1 promoter. Intracellular and extracellular fractions of transfected CHO cells were analyzed by Western blotting using the three anti-LEKTI antibodies (αD1-D6, αD8–D11, and αD13–D15 antibodies; Figure 1, lanes 3–5). Bands of 145 and 125 kDa were detected in the intracellular fraction of CHO cells transfected with pEF-DEST51-LEKTI$_{f\text{-}l}$ and pEF-DEST51-LEKTI$_{sh}$, respectively. These high-molecular-weight signals correspond to LEKTI precursors. They were not detected in the conditioned medium, indicating that proLEKTI is processed intracellularly, as observed in NHK. Using αD1–D6 antibodies, 10-, 13-, and 20-kDa fragments were detected in both the extracellular fraction of CHO transfected with pEF-DEST51-LEKTI$_{f\text{-}l}$ and pEF-DEST51-LEKTI$_{sh}$. These fragments are present in the NHK extracellular fraction (Figure 1, lane 2), and their size is consistent with LEKTI physiological cleavage. However, the 11- and 15-kDa fragments detected in NHK were not visualized in CHO extracts.

Using αD8–D11 antibodies, 20-, 31-, and 37-kDa bands were detected in the medium of CHO transfected with pEF-DEST51-LEKTI$_{f\text{-}l}$ and pEF-DEST51-LEKTI$_{sh}$ (Figure 1, lanes 3–5).

In addition, αD8–D11 and αD13–D15 antibodies (Figure 1, lanes 3–5) detected a 65-kDa fragment in the medium of CHO transfected with pEF-DEST51-LEKTI$_{f\text{-}l}$ and a 42-kDa fragment in the extracellular fraction of CHO transfected with pEF-DEST51-LEKTI$_{sh}$, as shown by Tartaglia *et al.* (2006).

As a result, heterologous expression of LEKTI$_{f\text{-}l}$ and LEKTI$_{sh}$ in CHO cells overall reproduces the proteolytic processing of LEKTI precursors seen in NHK and human epidermis. In addition, it provides evidence that both precursors are submitted to similar proteolytic processing, generating fragments of similar molecular weight. The only difference observed with the C-terminal fragments is due to the lack of D14 and D15 domains in the shortest precursor LEKTI$_{sh}$.

Furin Is a Key Enzyme for LEKTI Intracellular Proteolytic Processing

Subtilisin-like proprotein convertases (SPCs) are a family of endoproteinases involved in the processing of a variety of proproteins. Among them, furin has been proposed as a good candidate for the proteolysis of LEKTI (Bitoun *et al.*, 2003). To demonstrate the involvement of furin in LEKTI processing, pEF-DEST51-LEKTI$_{f\text{-}l}$ and pEF-DEST51-LEKTI$_{sh}$ vectors were used to transfect furin-deficient CHO cells. Intracellular and extracellular fractions were analyzed by Western blot using the three anti-LEKTI antibodies (Figure 2). In contrast to the various LEKTI proteolytic fragments visualized in the extracellular fraction of transfected CHO (Figure 2, lanes 1–3), no proteolytic fragment could be observed in the medium of transfected furin-deficient CHO cells (Figure 2, lanes 4–6). Instead, the 145- and 125-kDa LEKTI precursors were detected in the extracellular fractions of furin-deficient CHO cells transfected with pEF-

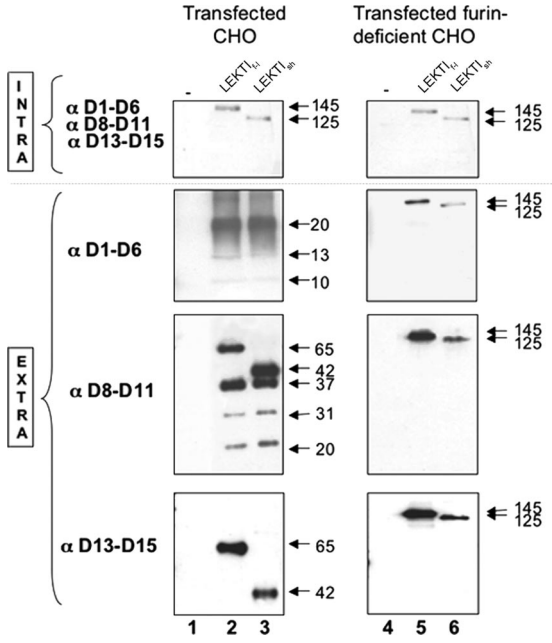

Figure 2. LEKTI processing involves a furin-dependant mechanism. Intracellular and extracellular extracts of CHO cells (lanes 1–3) and furin-deficient CHO cells (lanes 4–6) transiently transfected with the empty pEF-DEST51 vector (−, lanes 1 and 4); pEF-DEST51-SPINK5$_{f\text{-}l}$ (LEKTI$_{f\text{-}l}$, lanes 2 and 5); or pEFDEST51-SPINK5$_{sh}$ (LEKTI$_{sh}$, lanes 3 and 6) were analyzed by Western-blotting using anti-LEKTI antibodies indicated on the left. In both CHO cells and furin-deficient CHO cells, the 145- and 125-kDa LEKTI precursors are detected with each of the three anti-LEKTI antibodies in the intracellular fraction. However, in the extracellular fraction, LEKTI proteolytic fragments are visualized in CHO cells, whereas only LEKTI precursors are detected in furin-deficient CHO cells, with each of the antibody.

DEST51-LEKTI$_{f\text{-}l}$ and pEF-DEST51-LEKTI$_{sh}$, respectively, with each of the three antibodies used. These results showed that furin-deficient CHO cells are unable to process LEKTI, and that unprocessed precursors are secreted even so. Nevertheless, the furin-deficient CHO cells that we used were generated by ethyl methane sulfonate mutagenesis, and it is indeed possible that mutations elsewhere than in the furin gene could have occurred. To eliminate the possibility that such mutations were responsible for the lack of LEKTI processing, pEF-DEST51-LEKTI$_{f\text{-}l}$ was transfected in furin-deficient CHO cells stably retransfected with a murine cDNA of furin (Gu *et al.*, 1995). Extracellular fractions were analyzed by Western blot and revealed LEKTI processing rescue (Supplementary Figure 1). All together, these results prove evidence that furin plays a major role in LEKTI physiological processing.

Identity of LEKTI Fragments Inferred from Biochemical Analysis

To gain further insights into the identity of the diverse LEKTI fragments, we performed molecular weight analysis after deglycosylation experiments. The glycosylation site prediction servers NetNGly (http://www.cbs.dtu.dk/services/NetNGlyc/) and NetOGlyc (http://www.cbs.dtu.dk/services/NetOGlyc/) indicate the presence of two potential N-glycosylation sites on asparagine residues 505 and 763 located in D8 and D12 domains, respectively, and five O-glycosylation sites on threonine residues 1051, 1054, and 1055 and serine residues 1058, 1062, all located in the D15 domain (Figure 3A). N- and O-deglycosylation experiments were performed on NHK extracellular extracts and analyzed by Western blotting using the panel of antibodies. For N-deglycosylation experiments, PNGase F was incubated with NHK extracellular extracts (Figure 3B). O-deglycosylation of NHK extracellular protein extracts was performed by adding neuraminidase and *O*-glycosidase to the sample (Figure 3C).

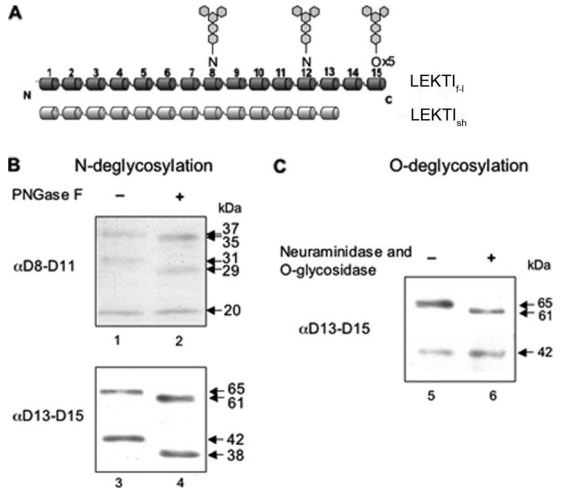

Figure 3. N- and O-glycosylation status of LEKTI proteolytic fragments. (A) Schematic representation of predicted N- and O-glycosylation sites on the full length (LEKTI$_{f\text{-}l}$) and the short length (LEKTI$_{sh}$) LEKTI precursors. N-glycosylation prediction involves two sites: one in the D8 domain, the other one in the D12 domain. Five O-glycosylation sites are predicted in the D15 domain. (B) Proteins from NHK conditioned medium were incubated in the absence (−) or presence (+) of PNGase F. After PNGase F treatment, the 31- and 37-kDa fragments recognized by the αD8–D11 antibody migrate at 29 and 35-kDa, respectively, whereas the 20-kDa band remains unchanged. Using the αD13–D15 antibody, C-terminal fragments of 42 and 65 kDa migrate at 38 and 61 kDa, respectively, when N-deglycosylated. (C) To assess O-deglycosylation, extracellular extracts of NHK were incubated at 37°C in the absence (−) or presence (+) of neuraminidase (1 h) and *O*-glycosidase (3 h). This treatment had no effect on the 42-kDa bands, but reduced the 65-kDa C-terminal fragment to a 61-kDa fragment.

As predicted by the software, no molecular-weight difference could be observed after any of these treatments when αD1–D6 antibodies were used (data not shown). On the basis of their molecular weights, some of these unglycosylated N-terminal fragments could correspond to single LEKTI domains D1, D5, or D6, previously identified (Magert *et al.*, 1999; Figure 1, right panel).

In contrast, when αD8–D11 antibodies were used, a 2-kDa shift of the 31- and 37-kDa bands was detected after N-deglycosylation. This treatment had no effect on the 20-kDa band (Figure 3B). No shift was observed for any of these three bands after O-deglycosylation (data not shown). The N-glycosylation result suggests that the 31-kDa fragment detected in epidermis and NHK correspond to LEKTI D8–D11 fragment (predicted molecular weight of 30 kDa). This is consistent with the description of the ~30-kDa fragment reported in NHK conditioned medium, the N-terminal of which corresponds to D8 (Ahmed *et al.*, 2001).

Finally, N-deglycosylation treatment resulted in a reduction of ~4 kDa of the 65- and 42-kDa fragments detected with αD13–D15 antibodies, demonstrating that these C-terminal fragments are N-glycosylated (Figure 3B). O-deglycosylation reduced the molecular weight of the 65-kDa C-terminal LEKTI fragment signal to 61 kDa, whereas the 42-kDa band was not affected (Figure 3C). This result is concordant with the O-glycosylation predicted sites on D15, which are absent from the shortest LEKTI isoform.

Each of the N- and O-deglycosylation experiment showed a 4-kDa shift of the 65-kDa fragment, revealing that this fragment carries several glycosylated residues accounting for 8 kDa. The molecular weight of the unglycosylated fragment (57 kDa) is concordant with the one calculated for the primary sequence of the last seven C-terminal domains of LEKTI (D9–D15), which is 57.4 kDa. To summarize, deglycosylation experiments lead us to propose that D1, D5, D6, D8–D11, and D9–D15 are physiological LEKTI domains derived from proteolytic processing of the full-length precursor.

LEKTI Domains, Except D1, Inhibit Epidermal Kallikreins

Based on the homology with other Kazal family members, LEKTI domains are predicted to inhibit serine proteases. In the Kazal family, the cognate protease is dictated by an amino acid occupying the P1 position.[1] Among all LEKTI domains, only D1, D2, and D15 do not possess an arginine at this position. Kazal inhibitor bearing an arginine at P1 position are known to inhibit trypsin. However, prediction is not simple because interactions between the inhibitory loop of the inhibitor and the active site of the inhibited protease also depend on the microenvironment of the complex. Moreover, the behavior of multidomain inhibitors toward their targets is not easily predictable.

To study the anti-protease function of physiological LEKTI fragments, we expressed recombinant LEKTI domains D1, D5, D6, D8–D11, and D9–D15. To provide evidence for the formation of disulfide bridges in the LEKTI

[1] The amino acid residues involved in the reactive site loop are numbered following the Schechter and Berger (1967) nomenclature.

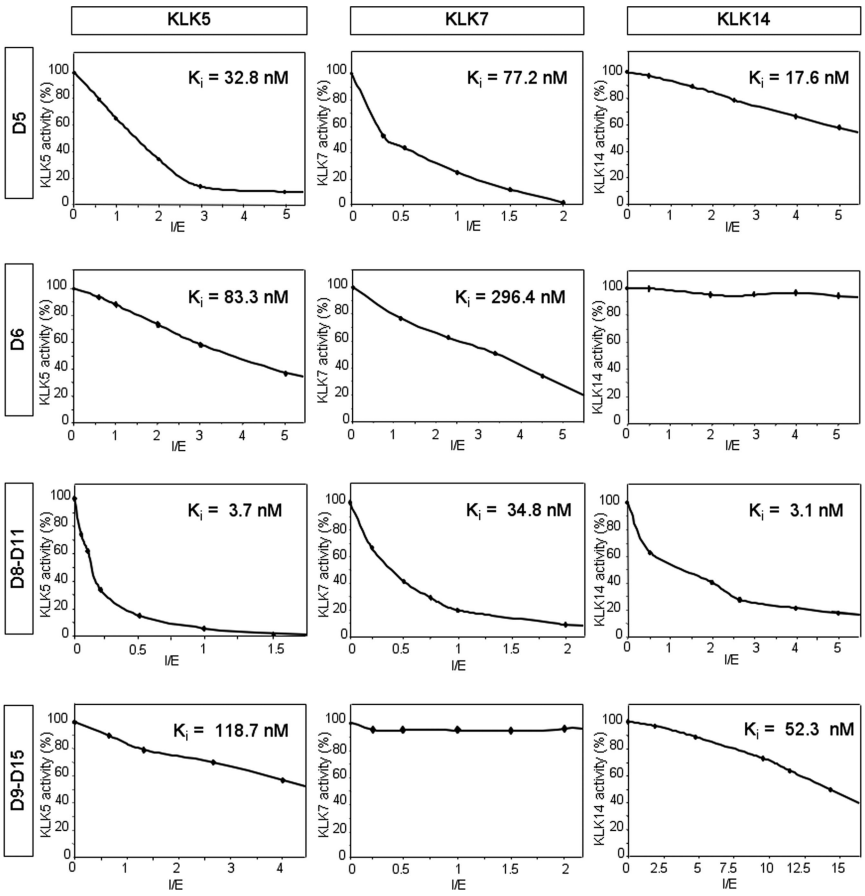

Figure 4. Inhibition properties of LEKTI domains toward epidermal kallikreins. Proteinases were incubated with increased concentrations of inhibitors before addition of substrates (described in Table 1). The curves represent the percentage of resulting proteolytic activity according to the ratio [inhibitor]/[enzyme]. Inhibition constants K_i were calculated as described in Materials and Methods. As illustrated by the slope of the curves, the D8–D11 LEKTI fragment is the most potent inhibitor of KLK5, KLK7, and KLK14. In contrast, D6 has no inhibitory property on KLK14, and neither has D9–D15 on KLK7.

fragments produced in prokaryotic expression system, these fragments were submitted to SDS-PAGE under reducing or nonreducing conditions (Supplementary Figure 2). After Coomassie staining, a single band was observed at the expected molecular weight with a slight difference between reducing and nonreducing conditions. This is consistent with the fact that the recombinant LEKTI fragments expressed in the Origami bacteria contained intramolecular disulfide bonds.

The capacity of purified recombinant LEKTI fragments to function in vitro as a serine protease inhibitor was then assessed against a large set of 13 serine proteinases involved in skin desquamation and inflammation: trypsin, tryptase, chymotrypsin, plasmin, thrombin, neutrophile elastase, cathepsin G, and kallikreins 1, 3, 5, 7, 8, and 14 (Table 1). Inhibition tests showed that the different LEKTI fragments were not equally effective against target proteinases: D1 was unable to inhibit any proteinase of the set, despite evidence for the formation of disulfide bridges (Supplementary Figure 2). In contrast, the other fragments inhibited trypsin, KLK5, KLK7, and KLK14 to various extents. The other proteinases tested in the panel were not inhibited by LEKTI fragments. The strongest inhibitory activity was observed with D8–D11 against KLK5 and KLK14 with K_i values of 3.7 and 3.1 nM, respectively (Figure 4). Despite a 68% sequence identity from the first to the fourth cysteine residues and an identical cysteine connectivity pattern, D5 and D6 differentially inhibited target proteinases. D6 appeared as a weaker inhibitor of trypsin, KLK5, and KLK7 than D5 and was not effective against KLK14. Specificity and capacity of inhibi-

Table 2. Summarization of inhibition constants and affinity constants

Protease	Substrate	Constants	D1	D5	D6	D8–D11	D9–D15
KLK5	HD-Ile-Pro-Arg-pNA	K_i (M)	—	32.8×10^{-9}	83.3×10^{-9}	3.7×10^{-9}	118.7×10^{-9}
		K_D (M)	—	9.3×10^{-10}	3.6×10^{9}	1.1×10^{-12}	9.5×10^{-1}
KLK7	MeO-Suc-Arg-Pro-Tyr-pNA	K_i (M)	—	77.2×10^{-9}	296.4×10^{-9}	34.8×10^{-9}	—
		K_D (M)	—	6.2×10^{-9}	6.7×10^{-8}	3.2×10^{-8}	nd
KLK14	IlD-Pro-Phe-Arg-pNA	K_i (M)	—	17.6×10^{-9}	—	3.1×10^{-9}	52.3×10^{-9}
		K_D (M)	—	nd	nd	nd	nd

For all LEKTI domains tested in this study, a summary of inhibition constants (K_i) and affinity constants (K_D) calculated from inhibition tests and BiaCORE analysis, respectively, is reported in this table. This report concerns the inhibited epidermal proteinases KLK5, KLK7 and KLK14. nd, not determined; —, no inhibition/no interaction.

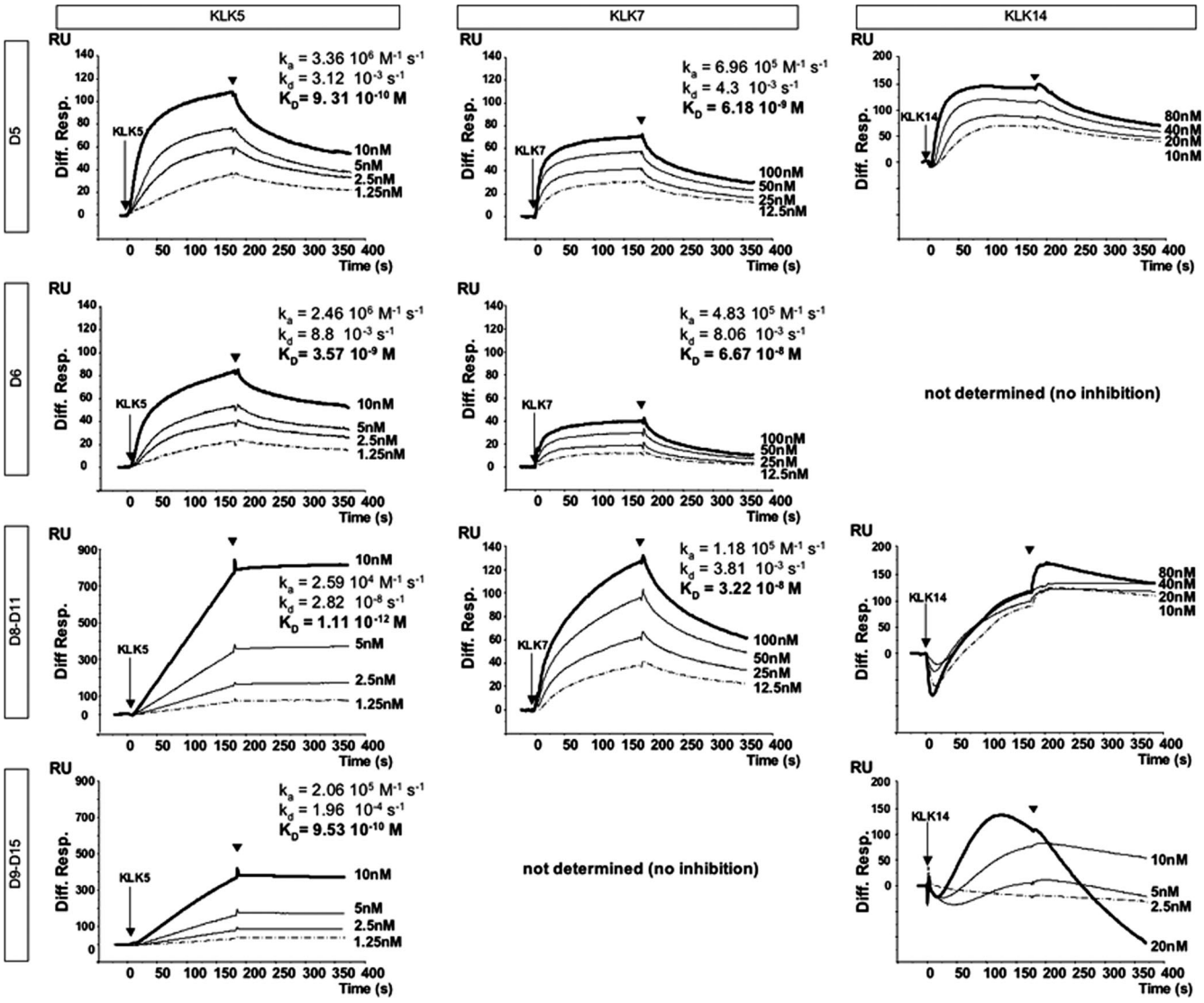

Figure 5. Surface Plasmon Resonance analysis of target proteinase binding to LEKTI fragments. LEKTI domains were immobilized onto a sensorchip. Proteinase solutions were injected over the sensorchip at concentrations ranging from 1.25 to 100 nM. Sensorgrams reflect binding during the association phase followed by the dissociation phase at the end of the injection. Representative sensorgrams show dose-dependent interactions of KLK5, KLK7 and KLK14 on D5, D6, D8–D11, and D9-D15 LEKTI domains. Each curve represents the specific interaction between the considered LEKTI fragment and proteinase. Raw binding data were analyzed using the BIAevaluation 4.0.1 software and fitted to obtain kinetics parameters. The kinetics constants k_a (association constant), k_d (dissociation constant), and K_D (affinity constant) are indicated on each graph. ▼, stop of proteinase injection and replacement with buffer; RU, resonance units; Diff. Resp., differential response.

tion of D6 are concordant with previously published data (Kreutzmann *et al.*, 2004; Egelrud *et al.*, 2005).

Despite the presence of an arginine at P1 position, which is associated with trypsin inhibition, three active LEKTI fragments (D5, D6, and D8–D11) were also able to inhibit KLK7, belonging to the chymotrypsin superfamily. Although full inhibition was achieved by adding D8–D11 at twofold molar excess to KLK7, D9–D15 was inactive even at 50-fold molar excess (data not shown). D8–D11 displayed a 10-fold lower inhibition capacity for KLK7 (K_i = 34.8 nM) compared with KLK5 (K_i = 3.7 nM). D6 was a poor inhibitor of KLK7 (K_i = 296 nM). Inhibition constants of each LEKTI fragment toward these epidermal proteinases are reported in Table 2. The results obtained with pancreatic trypsin were of the same order of magnitude as the one obtained with KLK5 (data not shown).

Dynamics of Interaction between LEKTI Fragments and Their Target Proteinases

The interaction parameters between LEKTI fragments and their target proteinases were determined using the SPR (BIAcore) technology (see *Materials and Methods*).

D1, D5, D6, D8–D11, and D9–D15 fragments were immobilized onto a sensorchip, and their binding capacity toward KLK5, KLK7, and KLK14 was tested in real time. The D1 LEKTI fragment, which was devoid of inhibitory capacity, was considered first. As expected, D1 was unable to bind any proteinase and was then considered to be a negative control in each BIA experiment.

Similarly to specific inhibition profiles of each LEKTI fragment, LEKTI fragments were not equally effective in their interaction capacities toward the tested proteinases (Figure 5).

As illustrated by sensorgrams, kinetics profiles and amounts of bound proteinase molecules were highly variable from one LEKTI fragment to another for each proteinase.

KLK5 exhibits different binding properties toward the four LEKTI domains. With single domains D5 and D6, the association phase as well as the dissociation phase occurs rapidly. This underlines a transient interaction between KLK5 and these single LEKTI domains. In contrast, the association phase between KLK5 and multidomain LEKTI fragments is slower, whereas the dissociation is less pronounced. Remarkably, after the injection of KLK5 is stopped, no dissociation from D8–D11 occurred. This reflects a high-affinity ($K_D = 1.11 \times 10^{-12}$ M) and irreversible binding of this complex. In contrast to KLK5, KLK7 dissociates very rapidly from D8–D11, as illustrated on sensorgrams by the decrease of bound molecules after the injection is stopped.

The interaction between single LEKTI domains D5 and D6 with KLK7 is weaker than the one determined with KLK5, as shown by their higher affinity constant (K_D) for KLK7. This difference is not due to their dissociation constants (k_d) toward KLK5 and KLK7, which are similar, but instead, to their weaker association constant (k_a) for KLK7 ($K_D = k_d \times 1/k_a$).

Sensorgrams of KLK14 interacting with different LEKTI fragments showed very particular profiles, different from those previously described for KLK5 and KLK7. Specifically for KLK14/D9–D15 interaction, the SPR signal abnormally decreased during the association phase before the end of injection, indicating a proteolytic activity of KLK14 against D9–D15. D9–D15 degradation was confirmed when KLK14 was injected at 20 nM and showed a loss of ligand immobilized during the dissociation phase, with a level of the SPR signal below the baseline. This phenomenon was less visible on the other sensorgrams but certainly occurred and prevented kinetic constant measurement.

pH Dependent–binding of KLK5 and LEKTI Is a Key Factor for the Regulation of the Desquamation Process

LEKTI and KLK5 are transported in different cargo vesicles before they are released into the extracellular space, at the stratum granulosum–SC interface. Immunoelectron microscopy experiments showed localization of the two molecules at this interface near corneodesmosomes in human skin (Ishida-Yamamoto *et al.*, 2005). KLK5 is a major proteinase involved in the desquamation process, through the cleavage of the corneodesmosomal components (Caubet *et al.*, 2004). To allow the detachment of the superficial layers of SC, KLK5 activity must be tightly controlled, in a spatially and temporally manner. Recent studies have suggested that the ultimate desquamation of corneocytes from the SC surface may be orchestrated by localized changes in pH (Elias, 2004; Hachem *et al.*, 2004). In this context, we analyzed the influ-

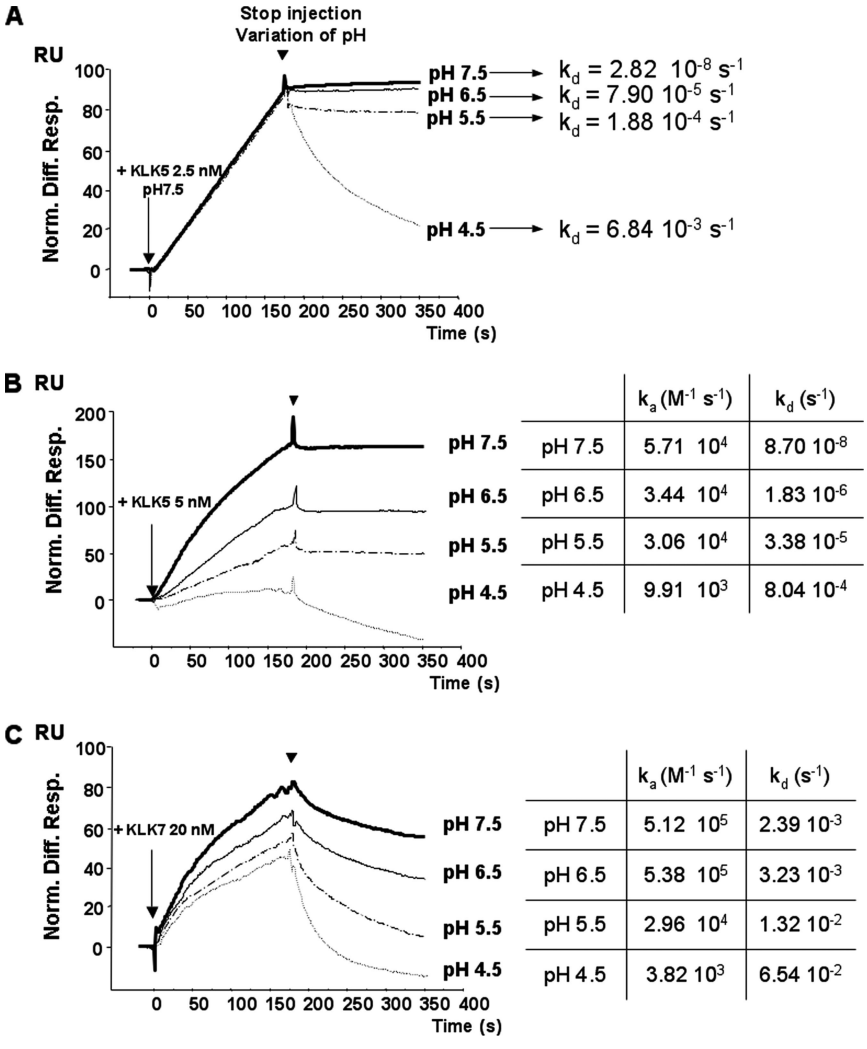

	k_a (M^{-1} s^{-1})	k_d (s^{-1})
pH 7.5	5.71 10^4	8.70 10^{-8}
pH 6.5	3.44 10^4	1.83 10^{-6}
pH 5.5	3.06 10^4	3.38 10^{-5}
pH 4.5	9.91 10^3	8.04 10^{-4}

	k_a (M^{-1} s^{-1})	k_d (s^{-1})
pH 7.5	5.12 10^5	2.39 10^{-3}
pH 6.5	5.38 10^5	3.23 10^{-3}
pH 5.5	2.96 10^4	1.32 10^{-2}
pH 4.5	3.82 10^3	6.54 10^{-2}

Figure 6. Effects of pH on the interaction between D8–D11 LEKTI fragment and target kallikreins, KLK5 and KLK7. (A) D8–D11 LEKTI domains were immobilized onto a sensorchip, over which KLK5 was injected at 2.5 nM in HBS-EP buffer at pH 7.5. At the end of the injection, this buffer was replaced by HBS-EP adjusted at various pH conditions varying from pH 7.5 to pH 4.5. The curves show D8–D11/KLK5 dissociation in response to pH changes. k_d values are indicated on the graph. (B and C) D8–D11 LEKTI domains were immobilized onto a sensorchip, over which 2.5 nM KLK5 (B) or 20 nM KLK7 (C) was injected in HBS-EP buffer at various pH values. Each curve represents the specific interaction between D8–D11 LEKTI fragment and the proteinase for each pH condition. The kinetic constants k_a (association constant) and k_d (dissociation constant) are indicated on the right of the sensorgrams. τ, stop of proteinase injection and replacement with buffer; RU, resonance units; Norm. Diff. Resp., normalized differential response.

ence of pH on the stability of KLK5 and D8–D11 interaction using the BIAcore technology (Figure 6). Injection of KLK5 at 2.5 nM was performed at pH 7.5, a pH occurring at the GR-SC interface. At the end of the injection, a buffer adjusted at different pH was injected, and the dissociation phase was followed for various pH conditions (7.5–4.5), miming the pH gradient in the SC layers from the depth to the surface. The sensorgrams presented in Figure 6A clearly show that the interaction between the two partners is affected by pH variable conditions, with an acceleration of the dissociation phase concomitantly with pH decrease. On release, both partners are potentially able to reform a complex at lower pH values. Therefore, the interaction (association and dissociation) was evaluated for each pH value (Figure 6B). The calculated values showed that the association decreases, whereas dissociation increases with acidification (pH 7.4 to pH 4.5). The effect is much stronger on dissociation (10^{-8} to 10^{-4} s^{-1}) than on association (10^{4} to 10^{3} M^{-1} s^{-1}). Therefore, acidification decreases the strength of binding between LEKTI D8–D11 and KLK5, by favoring dissociation of the complex. To test whether the binding between LEKTI D8–D11 and KLK7 was also pH-sensitive, we performed a binding experiment between these two partners at the same pH values (Figure 6C). Similarly, a decreased interaction was observed with acidification, with a high effect from pH 5.5.

pH changes influence the affinity between D8–D11 LEKTI fragment and its target proteinases. Therefore, we tested the inhibition capacity of D8–D11 against KLK5 and KLK7 at different pH values (Supplementary Figure 3). KLK5 and KLK7 activities were markedly decreased with acidification, but were still detected (20% activity at pH 4.5 compared with pH 7.5).

The highest inhibitory capacity for LEKTI D8–D11 was obtained at pH 7.5 and declined at inferior pH values, to become very weak at pH 4.5. This is concordant with the binding profile determined by BIA experiment and confirmed that the interaction and the inhibition capacity of LEKTI D8–D11 are optimal at neutral pH, which corresponds to the pH of the GR–SC interface. SC acidification allows active proteinases to be released from their inhibitor as a result of increased complex dissociation.

LEKTI Fragments Inhibit Native Epidermal Proteinases of the Stratum Corneum

To confirm the inhibitory capacity of D8–D11 toward disregulated proteinase activities in NS, in situ zymography was carried out on cryosections of *Spink5*$^{-/-}$ mouse skin. In situ zymography using fluorescein isothiocyanate (FITC)-conjugated casein as a substrate showed that proteinase activity was remarkably increased in the epidermis of *Spink5*$^{-/-}$ mice in comparison with WT epidermis (Figure 7B). This enzymatic activity mainly localized to the SC. Trypsin and chymotrypsin activities were then assessed with a synthetic substrate conjugated with AMC. Activities were markedly increased in the SC of KO mice compared with WT (Figure 7E,H). Addition of 5 μM D8–D11 LEKTI fragment on KO cryosection resulted in an important decrease in signal intensity (Figure 7, C, F, and I). The substrates (for trypsin and chymotrypsin) used in this study are preferentially cleaved by KLK5 and KLK7 (Debela *et al.*, 2006). However, we cannot exclude the possibility that other proteinase activities may degrade these substrates on skin cryosections.

To confirm the effect of the LEKTI D8–D11 fragment onto native KLK5 and KLK7, a casein gel zymography was performed (Figure 8). As already described in *Spink5*$^{-/-}$ epidermal extracts, KLK5 and KLK7 exhibited higher activities (Descargues *et al.*, 2005). The addition of LEKTI D8–D11

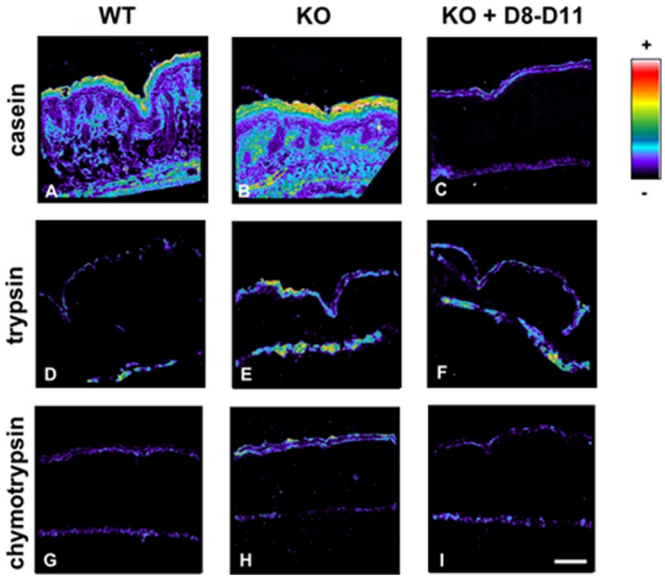

Figure 7. In situ zymography analysis. Protease activities were detected on skin cryosections from WT and *Spink5*$^{-/-}$ mice. The ability of D8–D11 LEKTI fragment to reduce these proteolytic activities was assessed on KO cryosections. (A) In WT epidermis, total protease activity detected by the degradation of the BODIPY FL casein substrate is mainly found in the SC. (B) In the epidermis of *Spink5*$^{-/-}$ mice, the caseinolytic activity is increased in the SC. (C) This activity is decreased in the presence of D8–D11 LEKTI fragment. (D and E) Trypsin-like activity detected by cleavage of the synthetic peptide Boc-Val-ProArg-AMC is increased in the SC of KO epidermis in comparison with normal epidermis. (F) Addition of D8–D11 LEKTI fragment decreases trypsin-like activity on KO frozen sections. (G and H) Incubation of frozen skin sections with the Suc-Leu-Leu-Val-Tyr-AMC peptide solution reveals that chymotrypsin-like activity is also markedly enhanced in the stratum corneum of KO epidermis, compared with WT. (I) These activities are decreased in the presence of D8–D11 LEKTI fragment. The color gradient represents the intensity values of the fluorescence signals ranging from dark to white. Bar, 50 μm.

completely abolished KLK5 activity, whereas a residual activity of KLK7 persisted. A 28-kDa protease also overactivated in KO epidermis was not affected by D8–D11. These results confirmed the involvement of D8–D11 LEKTI domain in the control of native KLK5 and KLK7 activities,

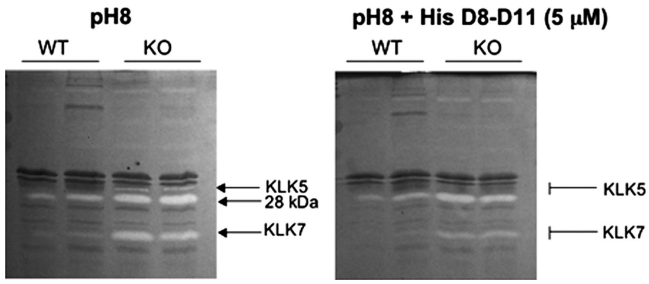

Figure 8. LEKTI D8–D11 inhibits native KLK5 and KLK7 activities in *Spink5*$^{-/-}$ mouse epidermal extracts. Epidermal extracts from 2 WT and 2 *Spink5*$^{-/-}$ animals were analyzed by casein gel zymography at pH 8 to detect proteolytic activity. Hyperactivity of KLK5, KLK7, and an unknown 28-kDa proteinase is observed in KO animals. Preincubation of the gel with D8–D11 LEKTI domain (5 μM) abolishes KLK5 activity and decreases KLK7 activity, and has little effect on the 28-kDa proteinase.

showing a stronger inhibition of KLK5, concordant with the inhibition data.

DISCUSSION

LEKTI is a Kazal-type multidomain protein composed of 15 potential proteinase inhibitor domains (Magert *et al.*, 1999). It is specifically expressed in the GR of the epidermis (Bitoun *et al.*, 2003). Absence of LEKTI expression is responsible for the severe skin disease NS. The study of NS patients as well as the analysis of a mouse model of NS provided evidence that LEKTI plays a key role in the control of the desquamation process (Descargues *et al.*, 2005, 2006). To gain further insights into the role of LEKTI in skin homeostasis, we first focused on the characterization of LEKTI active forms and carried out functional analysis of LEKTI fragments. In NHKs, we showed that LEKTI precursors are rapidly processed intracellularly into several proteolytic fragments, the molecular weights of which are concordant with single domains or several domains linked together. We showed that furin plays a major role in the generation of these proteolytic LEKTI fragments, which is concordant with immunolocalization of furin in the GR (Pearton *et al.*, 2001). In addition, the presence of 11- and 15-kDa N-terminal LEKTI fragments in the epidermis and in NHK that are not detected in CHO cells suggests that (an)other unidentified endoprotease(s) specifically expressed in keratinocytes could account for their production.

Once processed, all LEKTI proteolytic fragments are secreted in the conditioned medium of NHK. In human foreskin epidermis, LEKTI precursors are not detectable, in contrast to the numerous proteolytic fragments. These results indicate that LEKTI fragments, rather than LEKTI precursors, are the biologically relevant LEKTI forms, which are secreted at the GR-SC interface, as shown by immunoelectron microscopy (Ishida-Yamamoto *et al.*, 2005). Our study provides evidence for N- and O-glycosylation of LEKTI fragments. Protein glycans can play several roles (Lee *et al.*, 2001), including promoting protein folding into proper structure or protecting against proteolytic enzymes. The glycans present on LEKTI could then prevent the molecule from furin proteolytic action at sensitive sites in domain-linking regions. This could explain why LEKTI precursors are not processed into 15 domains as proposed (Komatsu *et al.*, 2002), but rather into several multidomain and single domain fragments.

Combination of Western blot analyses, molecular weight data, and glycosylation status lead us to propose the identity of some physiological LEKTI fragments. D1, D5, and D6 have been isolated from human blood; however, no cellular blood compartment has been shown to express LEKTI so far (Tartaglia-Polcini *et al.*, 2006). Therefore, D1, D5, and D6 circulating LEKTI fragments could originate from LEKTI-expressing tissues such as the epidermis and correspond to the smallest signals detected with αD1–D6 in the epidermis and NHK extracts. In addition to these single LEKTI domains, using internal and C-terminal antibodies, other LEKTI signals detected in the epidermis and in NHK were concordant with being new physiological LEKTI fragments corresponding to D8–D11 (31 kDa) and D9–D15 (65 kDa).

The physiological inhibition of proteinases depends on several parameters, including temporal and spatial colocalization of the protease and its inhibitor and binding kinetics between the partners involved. The goal of our study was to analyze the inhibitory capacity of the proposed physiological LEKTI fragments and to determine the associated kinetics parameters. In addition to pancreatic trypsin, among all proteases included in the panel studied, KLK5, KLK14, and KLK7 were the only proteinases inhibited by LEKTI fragments. Interestingly, these three proteinases are specifically detected in the GR of the skin and colocalize with LEKTI (Brattsand *et al.*, 2005; Ishida-Yamamoto *et al.*, 2005; Komatsu *et al.*, 2005). Each LEKTI fragment presents a specific inhibitory profile toward these three epidermal proteinases. D1 is devoid of inhibitory capacity as anticipated by its particular 3D structure (Lauber *et al.*, 2003). Except for this domain, the other fragments appear to have a higher inhibitory capacity toward trypsin-like proteases (KLK5, KLK14) compared with chymotrypsin-like proteases (KLK7). Surprisingly, whereas D6 inhibits KLK5, it is not active against KLK14, although KLK5 and KLK14 belong to the same family and share 65% similarity. This discloses a very fine specificity of interaction between Kazal domains and kallikreins.

Our results show that all LEKTI fragments studied, except D1, inhibit KLK5. D8–D11 demonstrated the highest inhibitory capacity with a K_i as low as 3 nM. This result correlates with the rapid and irreversible interaction occurring between the two partners. Although SPR technology did not allow determining the kinetics parameters of the interaction between KLK14 and LEKTI fragments, D5, D8–D11, and D9–D15 LEKTI domains displayed a high inhibitory capacity toward this proteinase. Taken together, these results identify KLK5 and KLK14 as the major targets of LEKTI fragments and KLK7 to a lesser extent. Using zymography analyses, we confirmed the inhibitory capacity of D8–D11 toward the native form of these epidermal proteinases.

Despite a high sequence homology (68%) between D5 and D6, D5 inhibits KLK14, whereas D6 does not. Structural studies of Kazal domain complexes reveal that there are 12 contact positions (P6, P5, P4, P3, P2, P1, P1′, P2′, P3′, P14′, P15′, and P18′) responsible for interactions between Kazal domains and their cognate serine proteinases (Lu *et al.*, 1997). Among these 12 contact positions, P4 and P6 are the only positions where the nature of residues differs between D5 and D6. At P6 position, a lysine is present in D5, whereas an arginine is found in D6. These two amino acids are structurally close and are not likely to explain the functional difference between the two domains. In contrast, the P4 position is occupied by a phenylalanine in D5 and by an alanine in D6. Interestingly, Empie and Laskowski (1982) found that substitution of a voluminous amino acid (Asp) in a small, and uncharged residue (Ala) at position P4 of Kazal ovomucoid third domain had a dramatic consequence on its inhibitory capacity toward trypsin-like enzyme subtilisin. Therefore, the difference of only 1 amino acid at P4 position between D5 and D6 LEKTI domains could account for their selectivity toward different serine proteinases.

This study highlights the specialization of LEKTI in the inhibition of epidermal proteinases KLK5, KLK7, and KLK14 and is consistent with an increased desquamation in NS patients. NS skin is also characterized by chronic inflammation, but the observation that inflammatory proteinases are not the direct targets of the studied LEKTI fragments suggests that KLK5 and KLK7 may have a proinflammatory role by activating PLA2 and IL1β, as proposed by Egelrud *et al.* (2005). Alternatively, it is also possible that additional physiological LEKTI fragments could have a direct activity against inflammatory proteinases.

The *Spink5*$^{-/-}$ mice revealed that LEKTI is a key regulator of the desquamation process through the control of KLK5 and KLK7 activities. In normal epidermis, LEKTI, KLK5, and KLK7 colocalize in the neighborhood of corneodesmosomes (Ishida-Yamamoto *et al.*, 2005). This suggests a finely regulated interaction between these partners to allow the detach-

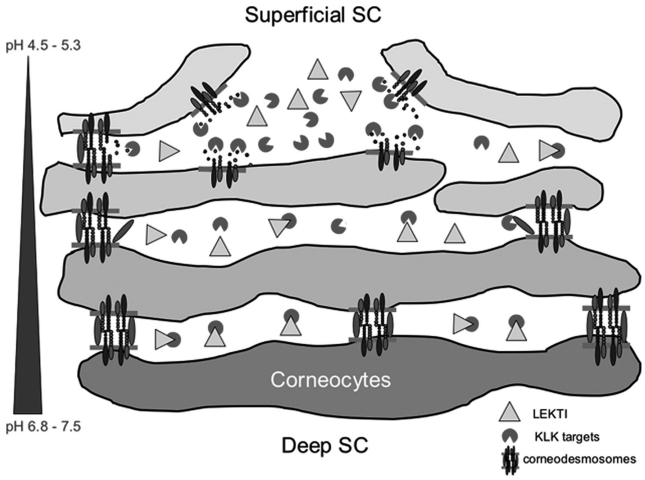

Figure 9. Model of desquamation: pH controls KLK activities by regulating their interaction with LEKTI. In the deep SC, neutral pH allows a strong interaction between LEKTI and its KLK targets in the corneocyte interstices, thus preventing corneodesmosomes cleavage. As the pH acidifies along the SC, LEKTI, and KLK5 dissociate, allowing proteinase to progressively degrade its corneodesmosomal targets. In the most superficial layers of SC, pH is low enough to ensure a strong dissociation between LEKTI and its KLK targets. The release of KLK inhibition, together with other proteinase activities, lead to complete degradation of corneodesmosomal components, resulting in the detachment of the most superficial corneocytes.

ment of the SC superficial layers only. Previous studies have demonstrated that pH is important for maintaining skin homeostasis and that transient increase in SC pH induces abnormality in permeability barrier (Hachem *et al.*, 2006). We mimicked the pH gradient occurring in SC layers during binding studies between KLK5 and D8–D11. At pH 7.5, the complex is very stable, but BIAcore analysis demonstrated that dissociation increases with acidification. The same effect of acidification could be observed on the dissociation rate of LEKTI–KLK7 complexes. This result is consistent with the possibility that during the passage of deep (pH 7.5) to superficial SC (pH 4.5) (Elias, 2004), KLK5 and KLK7 gradually dissociate from LEKTI. At acidic pH, KLK5 and KLK7 retain sufficient activity to degrade corneodesmosomal components, desmoglein-1, desmocollin-,1 and corneodesmosin (Caubet *et al.*, 2004). These results support the role of SC acidification in the control of the detachment of the most superficial corneocytes (Figure 9). The severity of the NS skin phenotype demonstrates the crucial need for a tight control of epidermal proteolytic activity. KLK5 and KLK7, as serine proteinases, display optimal activities at neutral pH, which is precisely the pH at the GR–SC interface. To prevent premature desquamation at the GR–SC interface, KLK5 and KLK7 activities must be strongly inhibited. This is consistent with the observation that the interaction between LEKTI and epidermal kallikreins is very strong at neutral pH. This highlights the importance of skin pH balance in the control of desquamation, acting at two levels: the control of protease activity, and the control of the interaction between proteinases and their inhibitors. All together, the resultant ensures an apparent proteolytic activity in a restricted environment.

This study is a base for an exhaustive analysis of inhibitory properties of all physiological LEKTI fragments. This will help to decipher the finely regulated balance between proteinases and their inhibitors in the context of the desquamation process.

ACKNOWLEDGMENTS

We are indebted to Dr. G. Zambruno (Laboratory of Molecular and Cell Biology, Instituto Dermopatico dell'Immacolata, IDI-IRCCS, Rome, Italy) for providing the anti-D13-D15 LEKTI antibody. We are grateful to Dr. S. Leppla for providing us with furin-deficient CHO cells and furin-transfected furin-deficient CHO cells. We thank Florence Capilla from the experimental histopathology platform of IFR30 (Génopole Toulouse Midi-Pyrénées) for technical assistance, as well as Sophie Allart from the cellular imaging platform of IFR30, Toulouse. We are grateful to Heather Etchevers and Jose-Enrique Mejia for critical review of the manuscript. This work was supported by grants from the national agency for research (ANR maladies rares), the French Ministry of Research and Technology, the French Foundation for Medical Research (FRM), the European Center of Skin and Epithelia Research (CERPER, Toulouse), and the European Geneskin coordination action project.

REFERENCES

Ahmed, A., Kandola, P., Ziada, G., and Parenteau, N. (2001). Purification and partial amino acid sequence of proteins from human epidermal keratinocyte conditioned medium. J. Protein Chem. *20*, 273–278.

Bitoun, E. *et al.* (2003). LEKTI proteolytic processing in human primary keratinocytes, tissue distribution and defective expression in Netherton syndrome. Hum. Mol. Genet. *12*, 2417–2430.

Brattsand, M., Stefansson, K., Lundh, C., Haasum, Y., and Egelrud, T. (2005). A proteolytic cascade of kallikreins in the stratum corneum. J. Invest. Dermatol. *124*, 198–203.

Caubet, C., Jonca, N., Brattsand, M., Guerrin, M., Bernard, D., Schmidt, R., Egelrud, T., Simon, M., and Serre, G. (2004). Degradation of corneodesmosome proteins by two serine proteases of the kallikrein family, SCTE/KLK5/hK5 and SCCE/KLK7/hK7. J. Invest. Dermatol. *122*, 1235–1244.

Chavanas, S. *et al.* (2000). Mutations in SPINK5, encoding a serine protease inhibitor, cause netherton syndrome. Nat. Genet. *25*, 141–142.

Debela, M., Magdolen, V., Schechter, N., Valachova, M., Lottspeich, F., Craik, C. S., Choe, Y., Bode, W., and Goettig, P. (2006). Specificity profiling of seven human tissue kallikreins reveals individual subsite preferences. J. Biol. Chem. *281*, 25678–25688.

Descargues, P. *et al.* (2005). Spink5-deficient mice mimic Netherton syndrome through degradation of desmoglein 1 by epidermal protease hyperactivity. Nat. Genet. *37*, 56–65.

Descargues, P., Deraison, C., Prost, C., Fraitag, S., Mazereeuw-Hautier, J., D'Alessio, M., Ishida-Yamamoto, A., Bodemer, C., Zambruno, G., and Hovnanian, A. (2006). Corneodesmosomal cadherins are preferential targets of stratum corneum trypsin- and chymotrypsin-like hyperactivity in Netherton syndrome. J. Invest. Dermatol. *126*, 1622–1632.

Egelrud, T., Brattsand, M., Kreutzmann, P., Walden, M., Vitzithum, K., Marx, U. C., Forssmann, W. G., and Magert, H. J. (2005). hK5 and hK7, two serine proteinases abundant in human skin, are inhibited by LEKTI domain 6. Br. J. Dermatol. *153*, 1200–1203.

Elias, P. M. (2004). The epidermal permeability barrier: from the early days at Harvard to emerging concepts. J. Invest. Dermatol. *122*, xxxvi–xxxix.

Empie, M. W., and Laskowski, M., Jr. (1982). Thermodynamics and kinetics of single residue replacements in avian ovomucoid third domains: effect on inhibitor interactions with serine proteinases. Biochemistry *21*, 2274–2284.

Gordon, V. M., Klimpel, K. R., Arora, N., Henderson, M. A., and Leppla, S. H. (1995). Proteolytic activation of bacterial toxins by eukaryotic cells is performed by furin and by additional cellular proteases. Infect. Immun. *63*, 82–87.

Gu, M., Rappaport, J., and Leppla, S. H. (1995). Furin is important but not essential for the proteolytic maturation of gp160 of HIV-1. FEBS Lett. *365*, 95–97.

Hachem, J., M.-Q.M., Crumrine, D., Uchida, Y., Roseeuw, D., Brown, B. E., Feigold, K. R., and Elias, P. M. (2004). Sustained increases in stratum corneum pH cause profound alterations in barrier functions and SC integrity. J. Invest. Dermatol. *122*, a167.

Hachem, J. *et al.* (2006). Serine protease signaling of epidermal permeability barrier homeostasis. J. Invest. Dermatol. *126*, 2074–2086.

Hewett, D. R., Simons, A. L., Mangan, N. E., Jolin, H. E., Green, S. M., Fallon, P. G., and McKenzie, A. N. (2005). Lethal, neonatal ichthyosis with increased proteolytic processing of filaggrin in a mouse model of Netherton syndrome. Hum. Mol. Genet. *14*, 335–346.

Ishida-Yamamoto, A. *et al.* (2005). LEKTI is localized in lamellar granules, separated from KLK5 and KLK7, and is secreted in the extracellular spaces of the superficial stratum granulosum. J. Invest. Dermatol. *124*, 360–366.

Jayakumar, A. *et al.* (2005). Consequences of C-terminal domains and N-terminal signal peptide deletions on LEKTI secretion, stability, and subcellular distribution. Arch. Biochem. Biophys. *435*, 89–102.

Jayakumar, A., Kang, Y., Mitsudo, K., Henderson, Y., Frederick, M. J., Wang, M., El-Naggar, A. K., Marx, U. C., Briggs, K., and Clayman, G. L. (2004). Expression of LEKTI domains 6–9′ in the baculovirus expression system: recombinant LEKTI domains 6–9′ inhibit trypsin and subtilisin A. Protein Expr. Purif. *35*, 93–101.

Komatsu, N., Saijoh, K., Toyama, T., Ohka, R., Otsuki, N., Hussack, G., Takehara, K., and Diamandis, E. P. (2005). Multiple tissue kallikrein mRNA and protein expression in normal skin and skin diseases. Br. J. Dermatol. *153*, 274–281.

Komatsu, N., Takata, M., Otsuki, N., Ohka, R., Amano, O., Takehara, K., and Saijoh, K. (2002). Elevated stratum corneum hydrolytic activity in Netherton syndrome suggests an inhibitory regulation of desquamation by SPINK5-derived peptides. J. Invest. Dermatol. *118*, 436–443.

Kreutzmann, P., Schulz, A., Standker, L., Forssmann, W. G., and Magert, H. J. (2004). Recombinant production, purification and biochemical characterization of domain 6 of LEKTI: a temporary Kazal-type-related serine proteinase inhibitor. J. Chromatogr. B Analyt. Technol. Biomed. Life Sci. *803*, 75–81.

Lauber, T., Schulz, A., Schweimer, K., Adermann, K., and Marx, U. C. (2003). Homologous proteins with different folds: the three-dimensional structures of domains 1 and 6 of the multiple Kazal-type inhibitor LEKTI. J. Mol. Biol. *328*, 205–219.

Lee, Y. R., Yamazaki, M., Mitsui, S., Tsuboi, R., and Ogawa, H. (2001). Hepatocyte growth factor (HGF) activator expressed in hair follicles is involved in in vitro HGF-dependent hair follicle elongation. J. Dermatol. Sci. *25*, 156–163.

Lu, W. *et al.* (1997). Binding of amino acid side-chains to S1 cavities of serine proteinases. J. Mol. Biol. *266*, 441–461.

Magert, H. J., Kreutzmann, P., Standker, L., Walden, M., Drogemuller, K., and Forssmann, W. G. (2002). LEKTI: a multidomain serine proteinase inhibitor with pathophysiological relevance. Int. J. Biochem. Cell Biol. *34*, 573–576.

Magert, H. J., Standker, L., Kreutzmann, P., Zucht, H. D., Reinecke, M., Sommerhoff, C. P., Fritz, H., and Forssmann, W. G. (1999). LEKTI, a novel 15-domain type of human serine proteinase inhibitor. J. Biol. Chem. *274*, 21499–21502.

Mitsudo, K., Jayakumar, A., Henderson, Y., Frederick, M. J., Kang, Y., Wang, M., El-Naggar, A. K., and Clayman, G. L. (2003). Inhibition of serine proteinases plasmin, trypsin, subtilisin A, cathepsin G, and elastase by LEKTI: a kinetic analysis. Biochemistry *42*, 3874–3881.

Morris, M. T., Coppin, A., Tomavo, S., and Carruthers, V. B. (2002). Functional analysis of *Toxoplasma gondii* protease inhibitor 1. J. Biol. Chem. *277*, 45259–45266.

Pearton, D. J., Nirunsuksiri, W., Rehemtulla, A., Lewis, S. P., Presland, R. B., and Dale, B. A. (2001). Proprotein convertase expression and localization in epidermis: evidence for multiple roles and substrates. Exp. Dermatol. *10*, 193–203.

Schechter, I., and Berger, A. (1967). On the size of the active site in proteases. I. Papain. Biochem. Biophys. Res. Commun. *27*, 157–162.

Schechter, N. M., Choi, E. J., Wang, Z. M., Hanakawa, Y., Stanley, J. R., Kang, Y., Clayman, G. L., and Jayakumar, A. (2005). Inhibition of human kallikreins 5 and 7 by the serine protease inhibitor lympho-epithelial Kazal-type inhibitor (LEKTI). Biol. Chem. *386*, 1173–1184.

Tartaglia-Polcini, A., Bonnart, C., Micheloni, A., Cianfarani, F., Andre, A., Zambruno, G., Hovnanian, A., and D'Alessio, M. (2006). SPINK5, the defective gene in netherton syndrome, encodes multiple LEKTI isoforms derived from alternative pre-mRNA processing. J. Invest. Dermatol. *126*, 315–324.

Traupe, H. (1989). The ichthyosis. A Guide to Clinical Diagnosis, Genetic Counselling, and Therapy, Berlin: Springer-Verlag.

Yang, T., Liang, D., Koch, P. J., Hohl, D., Kheradmand, F., and Overbeek, P. A. (2004). Epidermal detachment, desmosomal dissociation, and destabilization of corneodesmosin in Spink5−/− mice. Genes Dev. *18*, 2354–2358.